ELSEVIER

Earth and Planetary Science Letters 164 (1998) 535–551

EPSL

Magnetostratigraphy-based astronomical tuning of the early Pliocene lacustrine sediments of Ptolemais (NW Greece) and bed-to-bed correlation with the marine record

N. van Vugt [a,*], J. Steenbrink [b], C.G. Langereis [a], F.J. Hilgen [b], J.E. Meulenkamp [b]

[a] *Paleomagnetic Laboratory 'Fort Hoofddijk', Faculty of Earth Sciences, Utrecht University, Budapestlaan 14, 3584 CD Utrecht, Netherlands*

[b] *Department of Geology, Faculty of Earth Sciences, Utrecht University, Budapestlaan 4, 3584 CD Utrecht, Netherlands*

Received 12 January 1998; revised version received 7 October 1998; accepted 7 October 1998

Abstract

Continental deposits from the early Pliocene lacustrine Ptolemais basin in NW Greece display rhythmical alternations of lignite and marl beds. Three parallel sections from this area are studied using magnetostratigraphy and cyclostratigraphy. The presence of the greater part of the Gilbert Chron enables the recognition of astronomical periodicities in the succession. Especially the precessional influence is evident, as it determines the lithological cycles. The continental Ptolemais composite section is correlated to the most recent astronomical time scale — and thus to the marine reference section: the Rossello composite from Sicily [C.G. Langereis, F.J. Hilgen, The Rossello composite: a Mediterranean and global reference section for the Early to early Late Pliocene, Earth Planet. Sci. Lett. 104 (1991) 211–225] — on a bed-to-bed scale. It is concluded that lignite corresponds to an insolation minimum (beige layer in the Rossello composite), and marl to an insolation maximum (grey layer in the Rossello composite). This implies a precipitation increase during insolation maxima in early Pliocene continental Greece.

Keywords: magnetostratigraphy; fluvi lacustrine sedimentation; Pliocene; Mediterranean; lacustrine sedimentation

1. Introduction

Palaeoclimate and -environment reconstructions are a key to understanding modern climate changes, and geological deposits are a natural archive for past climate. The Milankovitch climatic periodicity, for example, can be recognised as cyclic patterns in the lithology of sediments. Hilgen [2] studied such patterns in Mediterranean Neogene marine records. Individual sapropels and carbonate cycles in the Trubi and Narbone Formations were correlated to precession cycles [3,4] and later to peaks in the summer insolation curve [5] using the La90 solution [6]. Shackleton et al. [7] obtained similar results in the Pacific Ocean by matching gamma-ray variations in deep sea cores to the Ber90 insolation time series [8].

For a better understanding of the climatic response to astronomical parameters, the continental record should be studied as well. Lacustrine sediments in particular can give valuable information on

* Corresponding author. Tel.: +31 30 253 5246; Fax: +31 30 253 1677; E-mail: vanvugt@geo.uu.nl

0012-821X/98/$ – see front matter
PII: S0012-821X(98)00236-2

the palaeoclimate and -environment, as demonstrated by Kent et al. [9] and Olsen et al. [10] in the Triassic Newark Basin. The sedimentary cycles they studied have frequencies similar to the present day values for astronomical variables. However, there is no reliable astronomical solution for the Triassic to establish a detailed correlation, nor is there a time-equivalent marine record to compare the climatic response with.

We have started an extensive programme to make bed-to-bed correlations between continental and marine sediments in the Mediterranean, in particular to the Rossello Composite [1], which is the basis for the Pliocene astronomical polarity time scale (APTS) [3–5]. One of the main goals of this programme is to reconstruct the palaeoclimate and -environment of the Neogene, both in the marine and continental realm. So far, we have focused on the lacustrine, rhythmically bedded lignite and marl alternations in Ptolemais, Northern Greece. The purpose of this article is to provide a magnetostratigraphic framework for the Ptolemais basin fill and, — with the cyclostratigraphic frame provided by Steenbrink et al. [11] — correlate the lithological cycles with the marine record and a suitable astronomical time series. Together with the sedimentological study and the $^{40}Ar/^{39}Ar$ ages [11] this will be the basis for further palaeoclimate studies on the Ptolemais area.

2. Geological setting

The elongated palaeolacustrine basin of Ptolemais is located between Florina and Kozani, approximately 100 km west of Thessaloniki (Fig. 1). It is part of a 250-km long graben system that opened in the Late Miocene and was divided into sub-basins in the Pleistocene [12,13]. Displacement along normal lystric faults related to this Pleistocene tectonic phase caused a bedding tilt of up to 15ºNNW. The basement consists of metamorphic schists in the west, and crystalline limestone in the east [14]. Large-scale lignite quarries in the eastern half of the basin provide expansive unweathered outcrops. The three studied sections are named after the pits in which they were located: Vorio, Komanos and Tomea Eksi (Fig. 1).

The basin fill has been divided into three formations: the Lower Formation, the Ptolemais Formation and the Upper Formation [15]. The Lower Formation overlies the crystalline basement, and is composed of lacustrine carbonate-rich marls. Only the top of this formation is exposed. The Upper Formation consists of fluvio-lacustrine marls with intercalated clay, sand and conglomerate beds.

Of main interest to this study is the Ptolemais Formation, that was dated as early Pliocene (Early Ruscinian, MN Zones 14 and 15) on the basis of palaeontologic data from small mammals ([16] and De Bruin, pers. comm.) and gastropods [17]. The Ptolemais Formation is subdivided into three members: the Kyrio, Theodoxus and Notio member (from bottom to top). The lowermost (Kyrio) member typically shows a rhythmic alternation of lignite and organic-rich grey marl beds, forming 30 lithological couplets with an average thickness of 2 m. In few localities, however, massive lignites without marl represent the Kyrio member. In the middle (Theodoxus) member, white marls alternate with thin lignites or dark grey organic-rich marls. One thick lignite layer divides this member in two. Because of the large lateral changes in bed-thickness and lithological expression, the rhythmic pattern is not as clear as in the other members. We estimate that there are six cycles with a typical thickness between 4 and 6 m each. The uppermost (Notio) member features nine of the same couplets as the Kyrio member, followed in one section by 11 couplets in which the lignite phase is represented by a dark brown clay bed, and in other sections by banded xylite. The couplets in the entire Ptolemais Formation can be recognised and correlated across most of the basin. Intercalated volcanic ash layers verify this correlation, and show that the rhythmic alternations are synchronous. They represent basin-wide lithological changes rather than lateral facies shifts [11]. We labelled the couplets in each member with a number, ascending towards the top (K1–30, T1–6 and N1–20).

The lithology of the Theodoxus and Notio members in the Komanos quarry differs from that in the two other sections. Starting gradually and laterally discontinuous from cycle K28 upwards, the lignites are replaced by thin brown horizons, and instead of grey marls we found beige marls lacking any organic material and with a loose, brittle texture. Samples from this part tend to break into little pieces shortly after retrieving them or during laboratory treatment.

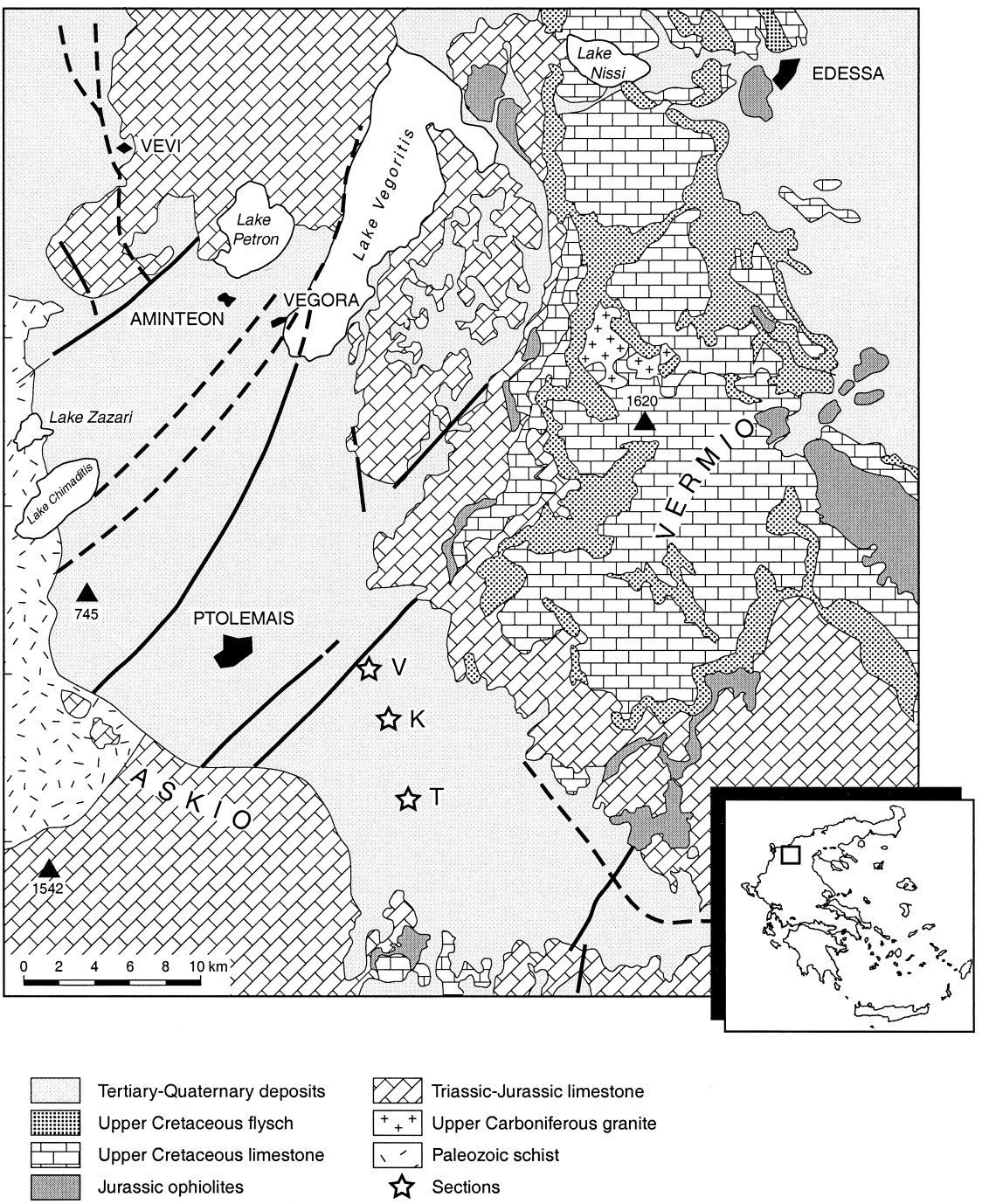

Fig. 1. Geological sketch map of the Ptolemais basin, *V* (*K*, *T*) is location of Vorio (Komanos, Tomea Eksi) section (after [37]).

The likely cause for this alteration is oxidation of the organic material during deposition of overlying layers.

Above cycle K13 in Tomea Eksi, the regular alternation is disturbed by lens-shaped layers cutting into the underlying sediment, indicating unconformities.

The first recognisable lithological cycle above this interval is K23. In Komanos, we find field evidence for a hiatus in approximately the same interval; a shallow scouring surface between cycles K18 and K19 is a sign for erosion, the thin palaeosol on top of this surface is interpreted as a period of non-deposition. For a more detailed (cyclo)stratigraphic description we refer the reader to [11].

3. Sampling and laboratory methods

The three parallel sections, Vorio, Tomea Eksi and Komanos, in the Lower and Ptolemais Formations were sampled for palaeomagnetic studies (see Fig. 1 for locations). An electrical drill was used to take oriented rock samples with a diameter of 2.5 cm. In the laboratory, these cores were cut into specimens with a length of 2.2 cm. The average stratigraphic distance between the sampling sites was 40 cm. Intervals around polarity reversals were later re-sampled with sampling intervals as small as 2 cm. Non-lignite lithology was preferred, because we knew from test samples that pure lignite does not give meaningful palaeomagnetic results. The outcrops in the mines were less than a year old, so hardly any digging was necessary to reach the unweathered rock. The lithology and thickness of the layers and the position and orientation of the samples were minutely recorded in field journals.

Bulk susceptibility was measured on a KLY-2 Kappa bridge. The natural remanent magnetisation (NRM) was measured on a 2G SQUID cryogenic magnetometer. Specimens with a negative (diamagnetic) susceptibility and an NRM below 10 μA m^{-1} were discarded because test samples did not give consistent magnetic directions in this situation. The lignitic samples were progressively demagnetised in an alternating field (AF) up to 125 mT. The other samples were thermally demagnetised with temperature increments of 30 and 50ºC, up to 570ºC. The delicate samples from the top of the Komanos section were exposed to alternating field treatment to prevent them from falling apart during demagnetisation. Twenty samples were progressively magnetised in a DC pulse field to acquire an isothermal remanent magnetisation (IRM). After each step, the remanence of the samples was measured on a JR5 spinner magnetometer. After saturation, the IRM was thermally demagnetised, and susceptibility was measured after each temperature increment.

4. Results

4.1. Magnetic properties

Many low-intensity samples did not give any sensible result, and were therefore discarded. The description of the characteristics of the remaining samples is divided in thermal and alternating field treatment.

Thermal demagnetisation generally reveals two non-viscous NRM-components (a viscous component is removed at 150–200ºC): a characteristic, normal or reversed component that decays towards the origin until ~390ºC, and a low intensity component that does not decay, but forms a cluster near the origin above ~500ºC (Fig. 2a), often in the direction west/down. The susceptibility increases at ~390ºC, and decreases again after ~520ºC. A small number of samples, with high intensities, have only one component above 200ºC, that reaches its maximum unblocking temperature at ~500ºC (Fig. 2b). Many samples show a large intensity decrease between 150 or 200ºC and 230ºC followed by no decay until 320ºC. This is caused by an exothermal reaction of the organic material in the rocks during heating. This reaction caused the samples to reach temperatures as high as 320ºC, although the furnace was set at 230º. Consequently, the intensity decreased according to the actual (higher) temperature, and no further decrease would occur in the next steps, until the previously reached temperature was exceeded. Around polarity reversals, some samples have a high temperature (HT) component (between 350–390 and 540ºC) with a polarity opposite to the lower temperature component (Fig. 2c). Although the unblocking temperature spectra generally overlap, the two polarities can be separated.

Alternating field demagnetisation shows two types of behaviour. In both types a viscous component is removed at 5–15 mT. The most common type I (Fig. 2d) reveals a single characteristic magnetisation that is fully demagnetised at 60/80 mT. Near reversals, the magnetisation sometimes contains two

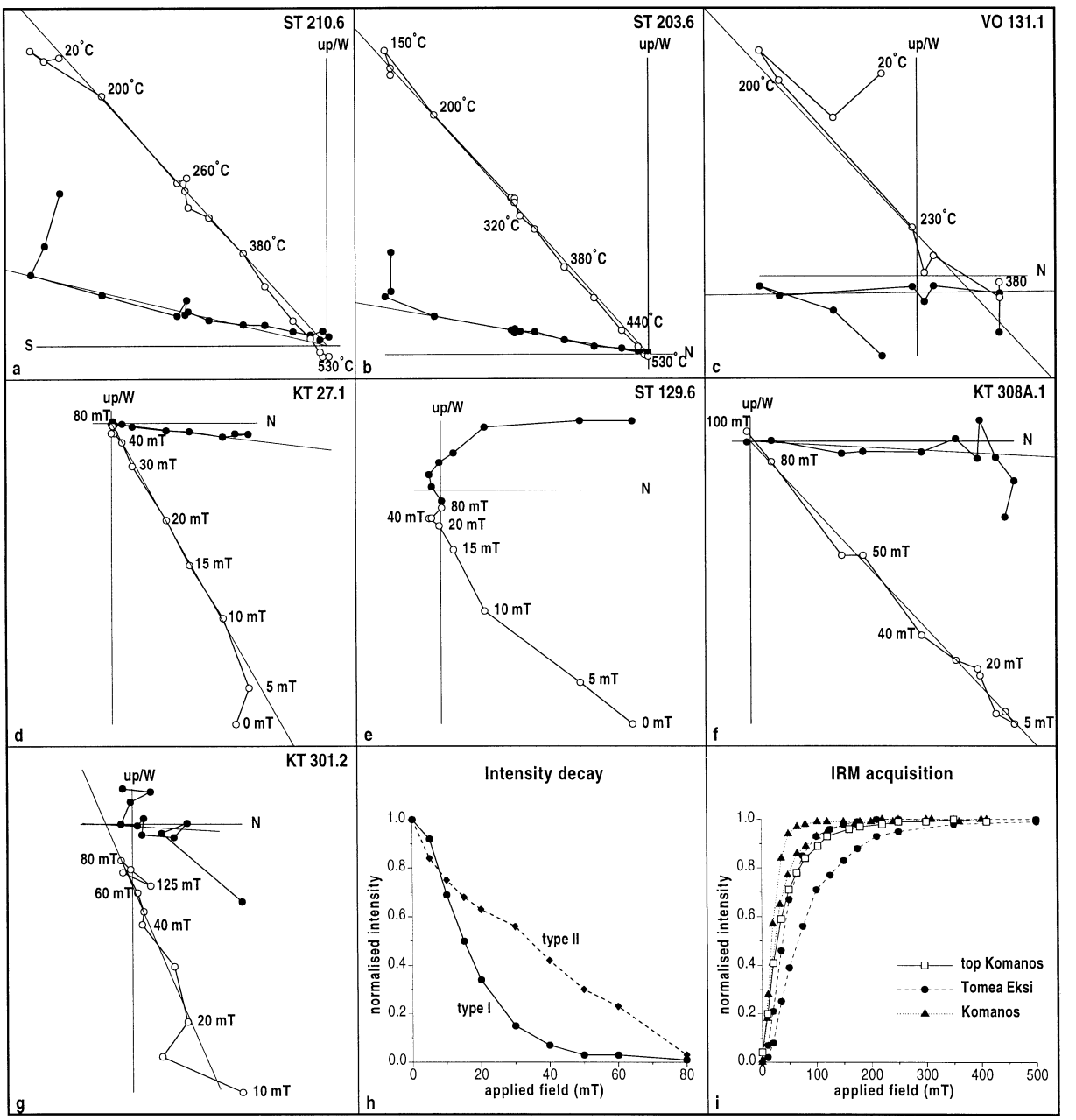

Fig. 2. Demagnetisation diagrams. Closed (open) circles denote the projection on the horizontal (vertical) plane. For details see text. (h) is an intensity decay curve during alternating field demagnetisation of a typical type I and type II sample (see text for discussion). (i) shows IRM acquisition diagrams of some characteristic samples. Typically, saturation is reached at fields of 100–200 mT; only occasionally higher fields (up to ~400 mT) are needed. The top part of Komanos consistently shows higher than average saturation fields.

components, a low coercivity (LC: 15–25/40 mT) and a high coercivity component (HC: 25–60/80 mT), with opposite polarities and overlapping coercivity spectra (Fig. 2e). The other type (II) only occurs in the Komanos section, and mainly in the top part of this section. The magnetic remanence is fully

demagnetised between 80 and 125 mT (Fig. 2f). Generally, only one component can be recognised in these samples, but occasionally two directions with opposite polarities can be seen (Fig. 2g). Type-I intensity–decay curves are concave, with a large intensity decrease at low coercivities and a small decrease at higher coercivities (Fig. 2h). The intensity of type II samples decreases more linearly (Fig. 2h).

In summary, samples with HT/LT (HC/LC) components with opposite polarities occur near reversals. In the same intervals, consecutive samples may have different polarities, even when they have only one component. This can only mean that these directions were not acquired simultaneously. Van Hoof and Langereis [18] described similar features in the marine Rossello composite section from Sicily. They concluded that their LT component was of earlier origin, whereas their HT component was acquired later, during early diagenesis. This 'delayed acquisition' was caused by cyclically changing redox conditions in the buried sediment. In Ptolemais, however, the pattern is not as consistent as on Sicily. Instead of one component carrying the earlier direction (LT), and the other the delayed one (HT), we find a seemingly random connection between the characteristics of a component (HT vs. LT or HC vs. LC) and its polarity. Nevertheless, the exact position of a reversal is determined by those intervals in which the HT and LT (HC and LC) consistently have the same polarity, meaning that a reversal is always positioned on top of an interval with mixed polarities.

Most samples reach IRM-saturation at fields between ~125 and ~200 mT, but saturating fields up to 500 mT are occasionally encountered (Fig. 2i). Together with the maximum unblocking temperatures and coercive forces, this indicates that (titano) magnetite and/or iron sulphides could carry the NRM. The type-II samples from the top of Komanos consistently saturate at higher than average fields (Fig. 2i), suggesting the NRM is carried by an oxidised magnetite.

4.2. Magnetostratigraphy

The magnetic directions derived from the demagnetisations are plotted versus stratigraphic level for each section, with respect to the cyclostratigraphic frame for the Ptolemais Formation (Fig. 3). The Vorio section reveals two normal polarity intervals, one in the lower half of the Kyrio member — containing the distinctive ash layer in cycle K7 — and one in the Notio member. In the middle part of Vorio, where the lithology consists of lignite only, both normal and reversed samples occur more or less at random; we regard the polarity pattern for this interval as inconclusive. In the Tomea Eksi section, we recognise the same two normal intervals. In addition, we find another two normal intervals in the middle (above K14) and top (around K23–28) of the Kyrio member. At the transition between the Theodoxus and Notio members we found no reliable data. All samples in the top 50 m of the Lower Formation (not completely shown in Fig. 3) recorded reversed polarity. In the Komanos section, we find a matching polarity pattern in the largest part of the Kyrio member, with the three normal intervals approximately around the same cycles (see also Table 1). In the top of the section, where the lithology and magnetic properties are different from those in the rest of the basin fill, the polarity pattern is not consistent with the two other sections. Based on field observations and analysis of the demagnetisation and IRM-acquisition diagrams, we suggest that the organic material has been oxidised after deposition and burial, thus changing the mineralogy. The newly formed or altered magnetic minerals in the sediment are then (re)magnetised and preserve a younger remanence, with possibly a different polarity. The palaeomagnetic results of the upper half of the Komanos section are therefore not used for the construction of a composite magnetostratigraphy.

Fig. 3. Palaeomagnetic results, polarity zones, stratigraphic names, cycle numbers and lithology of three Ptolemais sections. Closed (open) circles denote reliable (less reliable) characteristic components; triangles denote high-temperature or high-field components. In the polarity column, black (white) indicates normal (reversed) polarity, while shaded indicates undetermined polarity. In the lithological column, black (shaded) indented beds denote lignite (marly/clayey equivalent of lignite) beds, shaded (white) protruding beds denote grey (beige) marl beds; thin extra protruding layers denote volcanic ash layers and dark-shaded layers in the Kyrio Mb. in Vorio denote sand lenses.

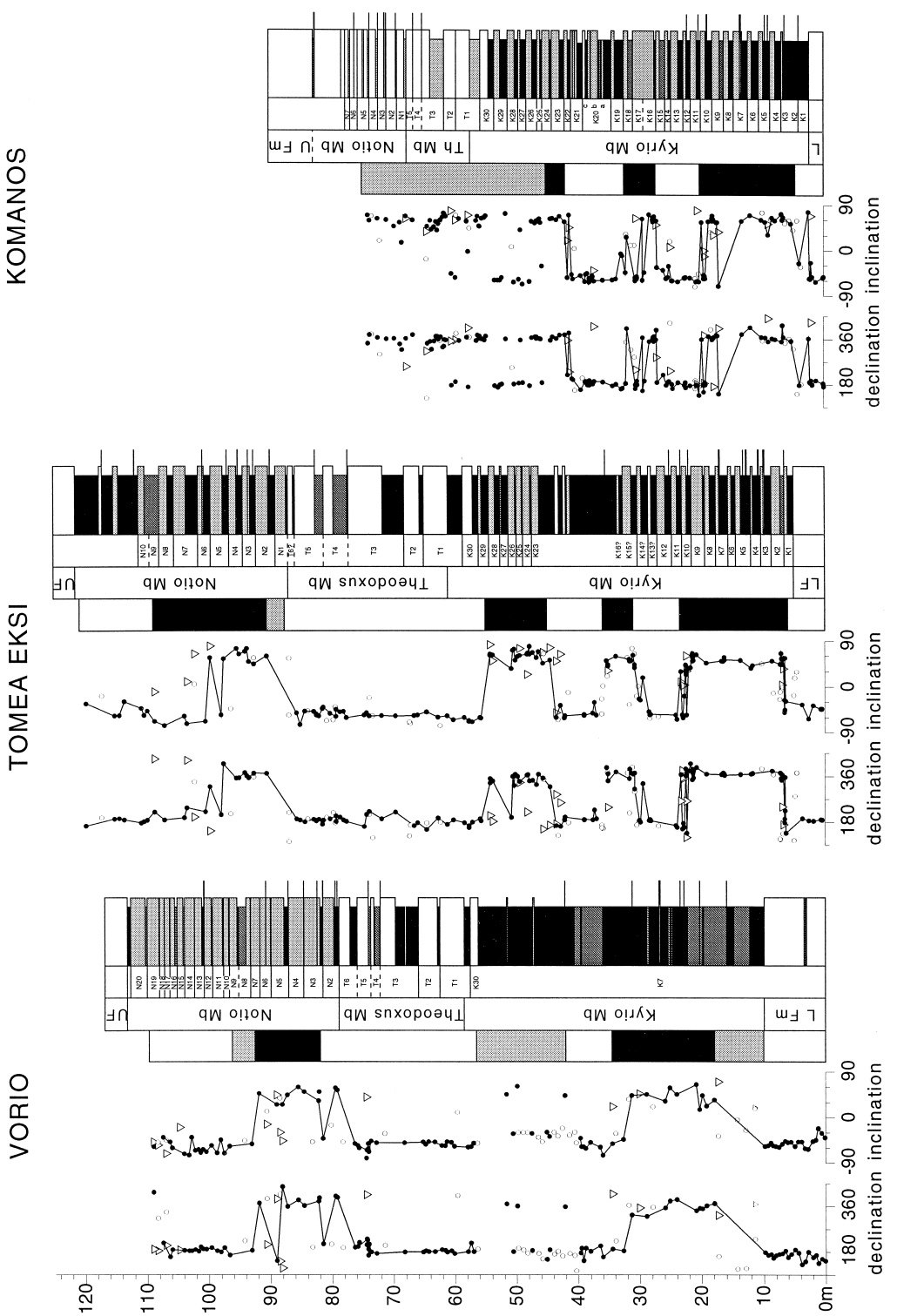
VORIO
TOMEA EKSI
KOMANOS
declination inclination
declination inclination
declination inclination
Notio Mb
Theodoxus Mb
Kyrio Mb
L Fm
U F
Th Mb
L
120
110
100
90
80
70
60
50
40
30
20
10
0m
180 360 -90 0 90

Table 1
Positions of the magnetic reversal horizons

	Vorio	Komanos	Tomea Eksi	Composite	i-cycle Ptol	i-cycle RC	Age (Ma)
U. Cochiti	mN7		lN9	lN9	403	403	4.188
L. Cochiti	mN3		lN1–lN2	mN3	414	413	4.300
U. Nunivak			lK29	lK29	433	433	4.493
L. Nunivak		mK22	below K23	mK22	446	445	4.632
U. Sidufjall		*top K18*	*above K16*	*top K18*	*464*	*460*	4.799
L. Sidufjall		lK16	lK15?	lK16	469	469	4.896
U. Thvera	?	base mK11	lK11	base mK11	478	478	4.998
L. Thvera	?	mK2/lK3?	lK2	lK2	497	500	5.236

Position of polarity reversals in the Ptolemais sections, K, T and N refer to the member; numbers refer to the cycle in that member; l and m refer to the phase (lignite or marl). Composite means the Ptolemais composite section; i-cycle Ptol (RC) denotes the insolation cycle correlated to the lithological cycle in which the reversal was found in the Ptolemais (Rossello composite) section. Ages of reversals after Ref. [5]. Italics denote the position of the hiatus rather than of the true upper Sidufjall reversal.

4.3. Ptolemais composite section

Through careful comparison of outcrops throughout the mining area, local features are separated from consistent (i.e. laterally continuous) patterns. These consistent cycle patterns are used to construct a cyclostratigraphic composite section for the Ptolemais basin (Fig. 5a), see Ref. [11] for details. The palaeomagnetic results of the different sections are integrated into a polarity pattern for the composite section. Because we find clear indications for delayed acquisition, we consider the position of each polarity boundary in the composite section to be at the highest (youngest) level with consistent polarity (Table 1).

The resulting composite Ptolemais magnetostratigraphy reveals four normal and five reversed intervals. Because the Ptolemais Formation was deposited during the early Pliocene ([16] and De Bruin, pers. comm.), there is only one option for correlation to the APTS [5]. Hence, the four normal intervals represent the Thvera, Sidufjall, Nunivak and Cochiti Subchrons in the Gilbert Chron (Fig. 4 and Fig. 5a).

With the palaeomagnetic reversals as age-calibration points, we can determine the average duration of the lignite–marl couplets. In Fig. 4a, the APTS is plotted versus the cumulative number of Ptolemais-cycles and their corresponding polarity. It appears that lines connecting consecutive reversals have similar slopes, with the exception of the Sidufjall and overlying reversed Subchron where the line is significantly less steep. The upper boundary of the Sidufjall, on top of cycle K18, coincides with the earlier mentioned unconformity. A scouring surface and palaeosol were interpreted as erosion and non-deposition respectively. If we assume a three-cycle gap at this point in the Ptolemais column, all the calibration points can be linearly correlated with a slope of 21.6 $\pm$ 0.5 kyr per couplet (Fig. 4b). Since this agrees very well with the average period of a precession cycle, we believe that the lithological cycles in Ptolemais are related to precession by its influence on the Mediterranean climate, as also found for the carbonate cycles in the marine Rossello record [4,5]. Independently from our method, a similar average duration of the lithological cycles in Ptolemais of 21.8 $\pm$ 0.8 was derived with $^{39}Ar/^{40}Ar$ dates [11].

5. Discussion

5.1. Correlation to an astronomical target curve

The next step is to correlate the Ptolemais-cycles to a suitable astronomical curve, e.g. climatic precession from the astronomical solutions Ber90 [8] or La90 [9]. Precession curves include the modulating effect of eccentricity and have proved successful in astronomical calibration of sedimentary cycles [3,4]. The precession index does not include the influence of obliquity, however, although obliquity is clearly reflected in marine lithological cycles. Early studies on Mediterranean sapropel sequences [19] used a monsoon index derived from a low-latitude insola-

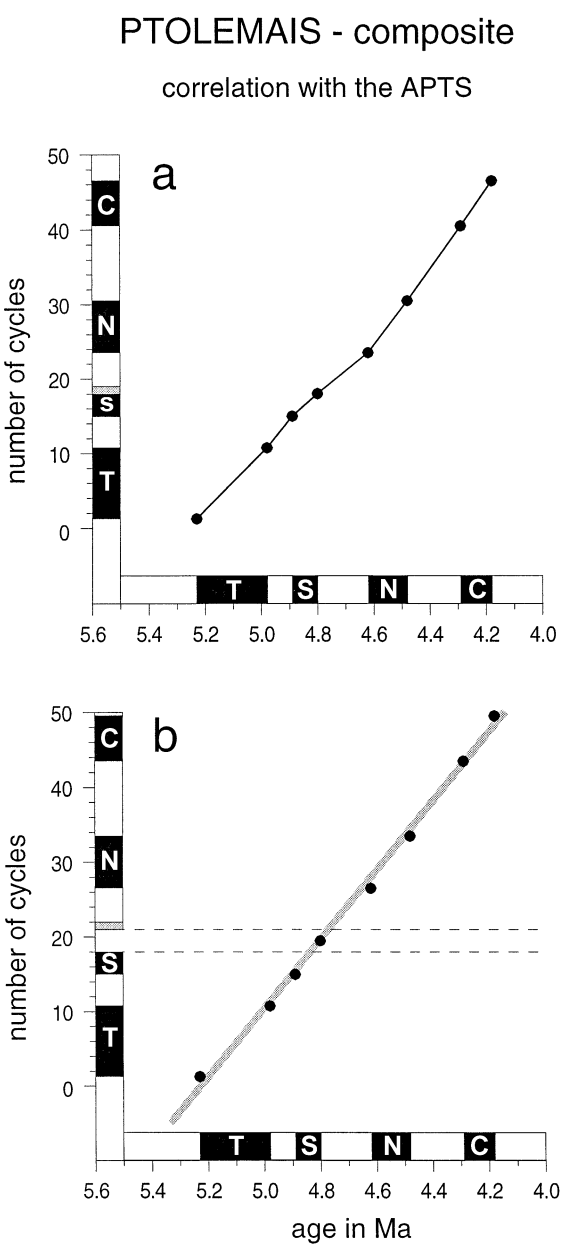

Fig. 4. Cumulative number of cycles in the Ptolemais composite section and their polarity versus the APTS. Black (white) denotes normal (reversed) polarity. T, S, N and C indicate the Thvera, Sidufjall, Nunivak and Cochiti Subchrons respectively. (a) There are clearly two linear segments through Thvera and Sidufjall, and through Nunivak and Cochiti, respectively. (b) Incorporating a 3 cycle hiatus allows a single linear correlation through all Subchrons.

tion gradient. More recently, Lourens et al. [5] suggested the use of 65ºN summer (average of June and July) insolation as a target curve, because it better expresses the influence of obliquity. They concluded that a consistency in phase relationships through the Pliocene and Pleistocene is best maintained using La90 with present-day values for both the dynamical ellipticity of the Earth and tidal dissipation. The 65ºN insolation is now generally used as a target curve for both mid and low latitudes [5,20–22]. The i-cycle codification of insolation peaks, introduced in Ref. [5], shall be used here for easy reference.

In Mediterranean sapropel sequences as well as in the carbonate cycles of the Rossello composite a maximum in summer insolation (warm summers and generally more precipitation) corresponds to a grey layer or a sapropel (both enriched in organic material), and a minimum in insolation (relatively cool summers and less precipitation) corresponds to a beige or homogeneous layer. This phase relation between Mediterranean marine lithology and insolation was determined by correlating the sapropels of the past 500 kyr with oxygen isotope stage boundaries as age calibration points [19,23] and by ^{14}C dating of the youngest sapropel in the Mediterranean ([24] and references therein). The Ptolemais Formation is of Pliocene age, and studies on modern basins in the area [25,26] did not (aim to) determine the modern continental or lacustrine equivalent of a sapropel. To derive an independent conclusion on a possible phase relation, we preferred not to make any a priori assumption. Therefore, we tried both option I: lignite corresponds to minimum insolation (beige or homogeneous layers in the marine record); and option II: lignite corresponds to maximum insolation (organic-rich layers in the marine record). Fortunately, option I was clearly more consistent and caused fewer discrepancies than option II, as is discussed below. This means that a lignite is correlated to a minimum in insolation (cool summers and generally arid) and marl to a maximum (warm summers and generally humid). This implies that the organic-rich layers in the Rossello composite are thus correlated with the relatively organic-poor layers (marl) in Ptolemais and vice versa.

A difficulty with Ptolemais is the lack of a straightforward cyclic representation of eccentricity, e.g. small and large scale clusters of precessionally

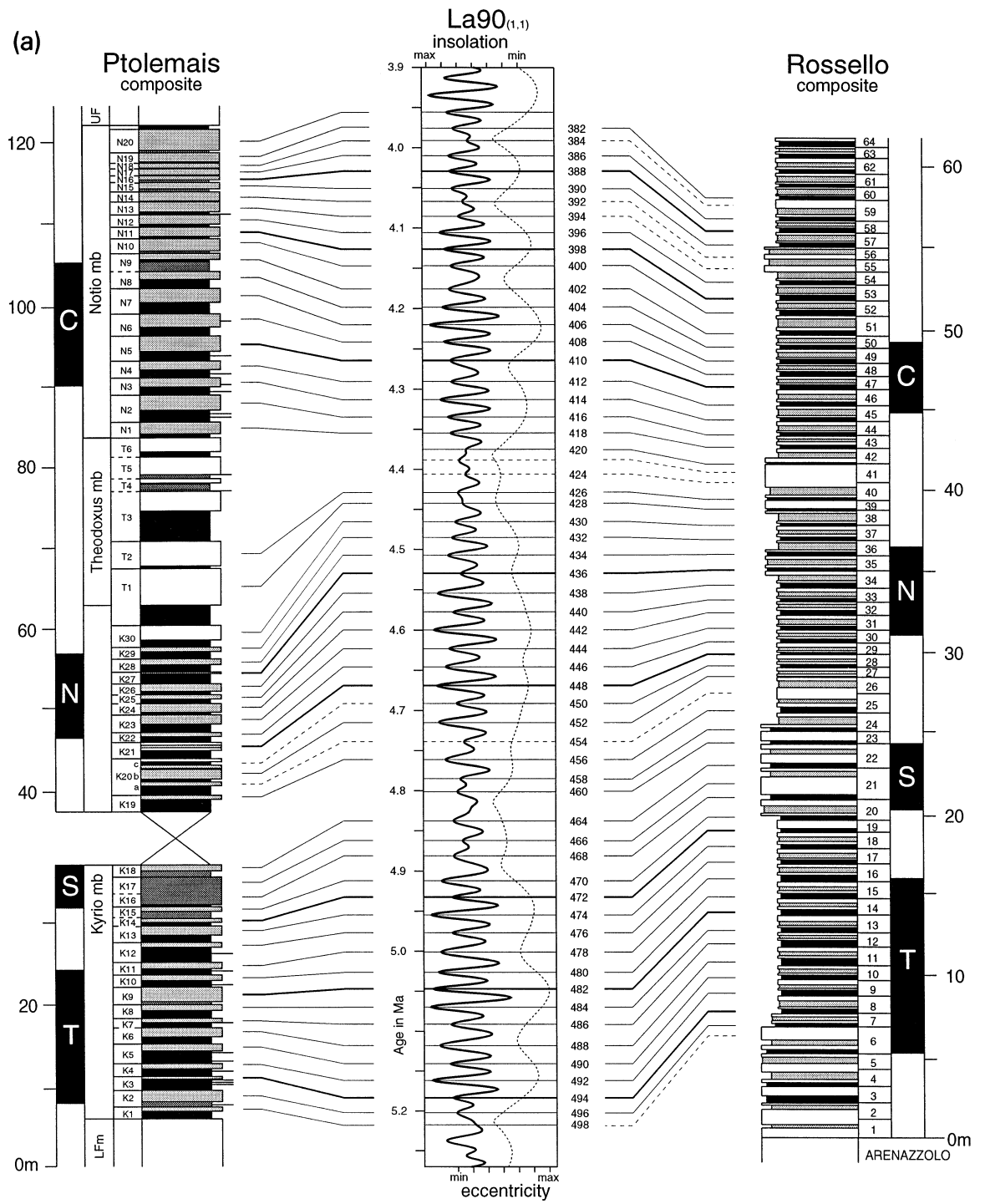

Fig. 5. (a) Magnetostratigraphy, stratigraphic names, cycle numbers and lithology of the Ptolemais composite section (see also caption to Fig. 3) correlated to 65ºN summer insolation, eccentricity (dotted) and the marine Rossello composite section; i-cycle codification of insolation peaks, indicated on the right hand side, after Lourens et al. [5]. *T*, *S*, *N* and *C* denote the Thvera, Sidufjall, Nunivak and Cochiti Subchrons respectively. In the lithological column of the Rosello section, black (shaded) indented beds denotes grey (beige) marls, and white protruding beds denote white carbonate-rich marls.

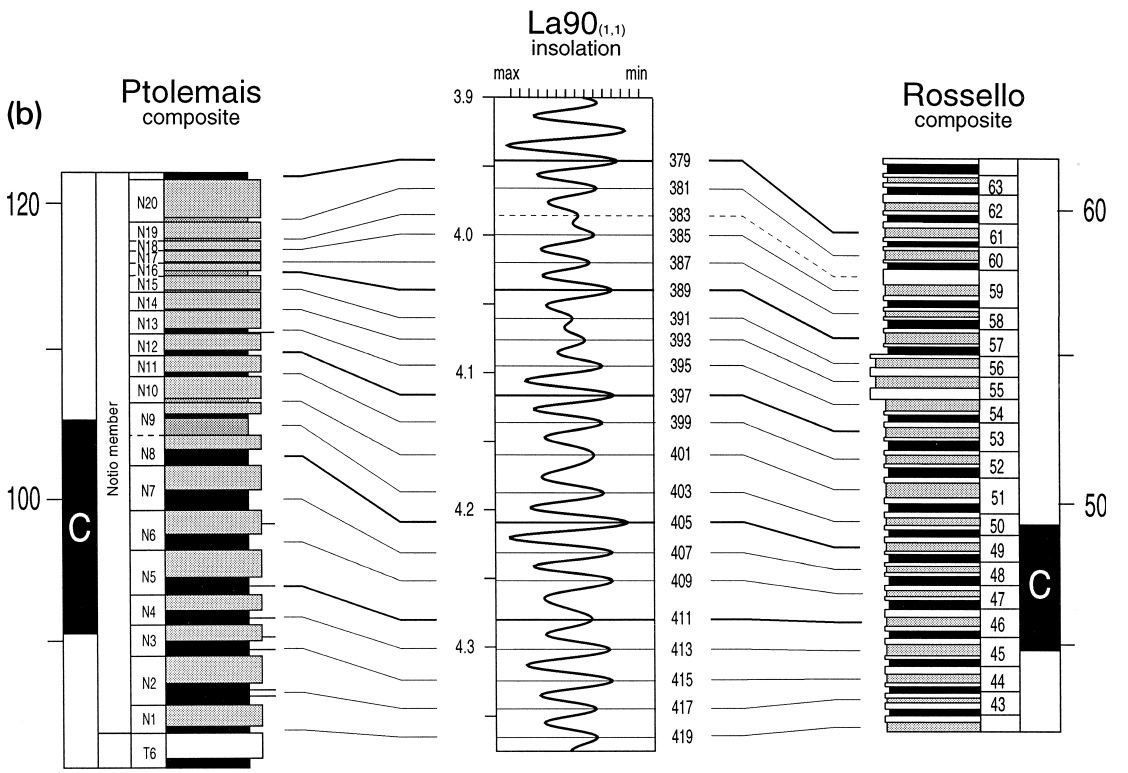

Fig. 5 (continued). (b) Enlargement of the tuning of the Notio member. Correlation lines connect lignites in Ptolemais, insolation minima and the corresponding beige layers in the Rossello composite.

forced cycles or a measurable quantity (e.g. carbonate content) that reveals the typical periodicities of eccentricity. Hilgen [3,4] used such observations to make a first (400-kyr eccentricity) and second (100-kyr eccentricity) order correlation to the astronomical target curve. In other cases (e.g. [7]), an age model for the geological record is constructed based on low-resolution features such as magnetostratigraphy and biostratigraphy. Such a model is then progressively refined and finally calibrated to an astronomical target curve. Our approach is based on the magnetostratigraphy of Ptolemais and the position of the corresponding reversal horizons in the astronomically calibrated Rossello composite. The time scale of Lourens et al. [5] correlates the Rossello section with the summer insolation time series. This time scale thus provides the approximate position of the Ptolemais reversal horizons with respect to insolation. This is only an approximate correlation because of possibly different delayed acquisition of the magnetic remanence between the Rossello and Ptolemais sections. Thus, the fact that a reversal horizon in the Rossello is correlated to a specific insolation cycle does not necessarily imply that the corresponding reversal in Ptolemais is found in the same insolation cycle.

We start our correlation where the lithological cycles are most pronounced: around the Cochiti Subchron in the Notio member and around the Thvera Subchron in the lower half of the Kyrio member. The polarity reversals provide a first order correlation to the insolation time series. The lithological cycles around the Cochiti Subchron, for example, should be recognised in the insolation pattern around ~4.25 Ma (Fig. 5a).

5.2. Tuning of cycles N1–19

The first eight cycles of the Notio member are very regular, but cycle N9 and the lignite phase of

N10 are not well developed (Fig. 5a, b). An alternation of thin lignite and marl layers represents these cycles in Tomea Eksi, while in Vorio a thin lignite and a dark clay can be recognised as the lignite phases of N9 and 10 respectively. Since cycle N1 contains the first regular lignite phase above the atypical Theodoxus member, this lignite is correlated to i-cycle 419, i.e. the first insolation minimum with a relatively high amplitude after a series of low-amplitude oscillations (caused by a 400 kyr eccentricity minimum). In the Rossello section a transition from double, high-carbonate cycles (Rc 40–41) to regular cycles occurs at the same level (Rc-cycle 42). Cycles N2–8 are then correlated to consecutive insolation peaks, and cycle N9 and the lignite of N10 to the moderate amplitude insolation peaks 403–401. The marl of cycle N5 is in most outcrops thicker than average and its top half often contains numerous thin lignite beds. In our correlation, this marl corresponds to i-cycle 410, an insolation maximum with a relatively long duration.

The uppermost cycles of the succession (N10–20) are dominated by marl and can only be distinguished by their thin lignite phases that are occasionally represented by brown clay layers rather than real lignite (Fig. 5b). The lignite phases of N10, 14, 15, 17 and 19 are represented by thin clay layers; while N11, 12, 13, and also N16 and N21 have relatively thick lignites or dark clays. This pattern fits excellently with the high-amplitude minima 399, 397, 395 and with 389 and 379 and the lower amplitude cycles in between. The relatively dark N14-marl and the thin N18-marl are now correlated to the low-amplitude maxima 392 and 384 respectively. The only significant inconsistency with the Rossello-composite pattern is the thick beige layer in Rc 51: its equivalent is a thin dark clay layer (lignite-phase of N10), correlated with a low-amplitude, long-duration insolation minimum (401).

5.3. Tuning of cycles K1–18

The Kyrio member has fairly constant and regular cycles up to cycle K14, except for the first two cycles (K1–2). Although cycles K1 and 2 are developed in Tomea Eksi only, and therefore their expression may just represent a local phenomenon, it appears that K1 has an ordinary lignite, while its marl and the overlying lignite of K2 are merged into an alternation of thin layers of lignite and marl. Despite the lack of lateral continuity, it is remarkable that the pattern of these two cycles followed by a long series of regular cycles fits very well with the insolation pattern near the 400 kyr eccentricity minimum at 5.22 Ma. Cycles K1 and K2 are thus correlated to i-cycle 499/498 and 497/496 respectively, and the overlying cycles K3–14 to insolation peaks 495–472. The only inconsistency is cycle K9, which has, despite the regular overall thickness, a relatively thin and less pronounced lignite, overlain by a thicker marl. The transition between the lignite and the marl is gradual, and an erroneous position of this boundary may explain the different thickness ratio. It remains conspicuous, however, that in our correlation this less pronounced lignite K9 corresponds to the highest amplitude insolation minimum between 4 and 5 Ma (i-cycle 483), especially since this cycle is not prominent in the Rossello composite section (Rc 13).

The lignite phases of cycles K15 and 18 contain many thin marl beds, while K17 does not even have a lignitic interval. The thickness of the combined marl bed of K16–17 led to the interpretation of K17 as a separate cycle. The less pronounced or absent lignites in this interval are correlated to the low amplitude insolation minima connected with the eccentricity minimum at 4.9 Ma. Similar considerations for the marl beds (the intercalation of thin lignite layers throughout the marl of K16–17) lead to correlation to the low amplitude i-cycles 468–466. Supportive for this correlation are the similarities between the cyclic patterns of the Ptolemais and Rossello sections. The absent beige layers in Rc 19 and double cycle Rc 21 in the Rossello composite correspond very well to the less pronounced lignite K15 and absent lignite K17 in Ptolemais.

5.4. Tuning of cycles K19–30

With the detailed correlation so far, the reversal horizons corresponding with the upper Thvera and lower Sidufjall as well as with the upper and lower Cochiti in Ptolemais coincide with those in the Rossello composite section (and thus with the reversals in the APTS) within an interval of less than one cycle (or less than 21 kyr) (Table 1). It seems therefore reasonable to expect the same small differ-

ence for the Nunivak reversal horizons, even despite a possible difference in delayed remanence acquisition. The most remarkable feature in the Nunivak interval is the very thin or sometimes even absent marl of cycle K27. Either insolation maximum 436 (with very low amplitude) or 440 (with relatively low amplitude, caused by the high amplitude of neighbouring maxima 442 and 438) is the best candidate for correlation to cycle K27. The marl of K25 is also thinner than average, and marl K29 was found to be very thin in Tomea Eksi, but average in Komanos and in a (not published) outcrop near the Vorio field. For the equivalent of a high-amplitude insolation maximum (438 and 442) we expect a marl enhanced in thickness and/or in appearance. Marl K24 has both, marl K26 is thicker than average, and marl K28 is in some outcrops enhanced, in others not. Altogether, the preferred correlation for this interval connects thin or absent marl K27 to the lowest-amplitude maximum 436, which means that enhanced marls K24 and K26 are correlated to high-amplitude maxima 442 and 438 respectively, and marls K25 and K29 to i-cycles 440 and 432 respectively. The correlation is extended straightforwardly downwards to cycle K21 and upwards to K30.

For the interval K19–20, the correlation with the insolation time series is not unambiguous, because there is no distinct or typical cyclic pattern, and the connection with underlying cycles is disturbed by the inferred hiatus. While cycle K19 appears to be a regular cycle, K20 has a thick heterogeneous marl phase and might be composed of two or even three cycles. We estimated earlier that the hiatus probably represents three cycles. Exactly three insolation cycles above the insolation maximum (i-cycle 464) correlated to the uppermost marl below the hiatus, K18, a prominent, normal-amplitude insolation cycle is present (i-cycles 457–456). We correlate K19 to this cycle. That leaves three cycles for K20, of which the upper- (450) and lowermost (454) maxima and the lowermost minimum (455) have reduced amplitude. For reasons of consistency cycle K20 is thus divided into three cycles (a, b and c), and correlated to the three insolation cycles. Considering the appearance of this interval in the Rossello composite (Fig. 5a), where i-cycle 454 lacks expression, we suggest that the marl of K20a might be absent, and that the increased number of thin lignite layers just below the top of the thick marl phase of K20 marks lignite K20c.

5.5. Tuning of cycles T1–6

The Theodoxus member is now confined to the insolation peaks between i-cycles 429 and 420. As mentioned earlier, the bed thickness is laterally variable; a metres thick marl layer can disappear over a distance of only 100 m. The only constant beds are thin lignite T2, thick lignites T1 and T3 and the two ash layers in cycles T4 and T5. The extraordinarily thick lignite of T3 is correlated to the relatively high-amplitude minimum 425. T1 and T2 are thus necessarily correlated to the double insolation maximum 426–428 and the upper part of the Theodoxus member should correspond to the remaining two and a half insolation cycles. This upper part, however, was interpreted as three and a half lithological cycles (marl phase of T3 and T4–6), but the cyclic pattern is difficult to recognise in this particular interval. In the Rossello composite, the beige layer (Rc 40) corresponding to the extra thick lignite T3 is very thick, while the beige below (Rc 39) is absent. The number of cycles in the Rossello-equivalent of cycles T3–6 corresponds to the number of insolation peaks, although these (double) cycles are again difficult to recognise.

5.6. Alternative correlation of cycles K19–T6

To explore the discrepancy between the number of insolation peaks and the apparent number of lithological cycles in the Theodoxus member, an alternative correlation has been examined (Fig. 6). In this alternative correlation, all lithological cycles between K19 and T6 are correlated to two insolation cycles older than in the previously discussed correlation.

The marl of thick cycle T3 is correlated to the double insolation maximum 426–428, introducing one extra lithological cycle. I-cycle 425 should then represent an enhanced lignite phase, but it does not. The marls of K29 and K28 (both with varying thickness) are then correlated to the lowest-amplitude maximum 436 and to the high-amplitude maximum 438 respectively, and the enhanced marl of K24 is correlated to the relatively low-amplitude i-cycle 446. When this alternative correlation is extended

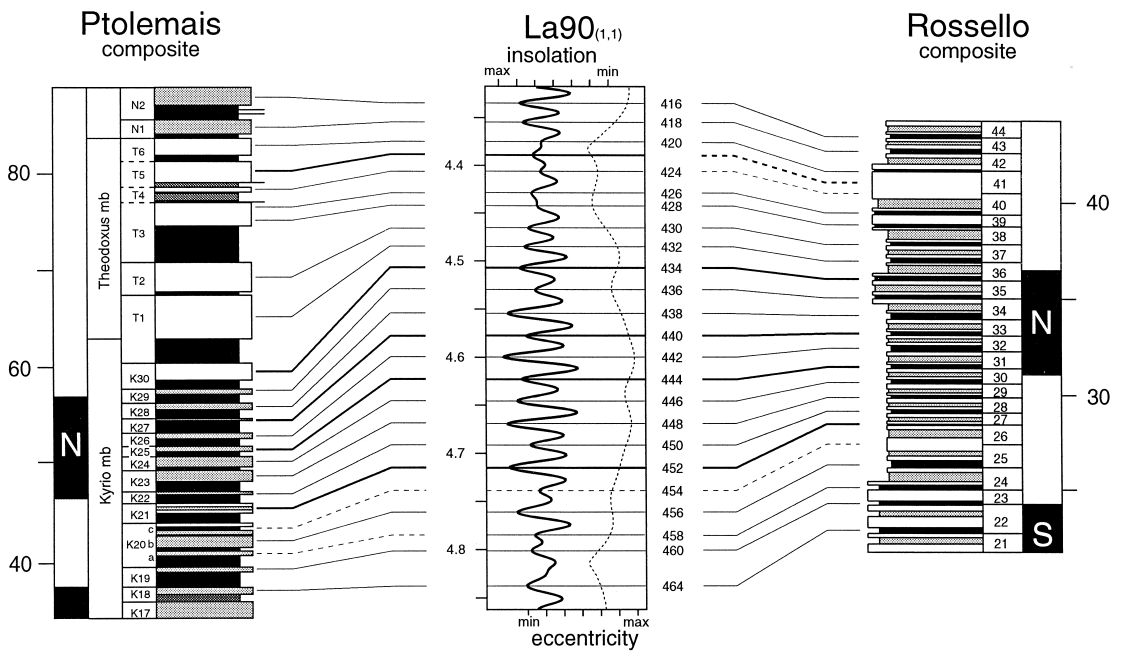

Fig. 6. Alternative correlation in the interval 4.6–4.4 Ma. The tuning of cycles to insolation is only slightly less consistent than in the preferred correlation, but a major disparity with the Rosello composite is introduced by the discrepant position of the Nunivak reversal boundaries. See also caption to Fig. 5a.

downwards, assuming that cycle K20 indeed represents three insolation cycles, it follows that the hiatus between K18 en K19 is reduced to one (low-amplitude) insolation cycle (463/462). Since, moreover, this insolation cycle could well be incorporated in K19, the hiatus would be eliminated.

In addition to the inconsistencies between the lithological and insolation pattern, the alternative correlation makes the Nunivak Subchron significantly too old. This can only be explained by a two-cycle delayed acquisition of magnetic remanence in this specific interval in the Rossello composite, which is unlikely considering the consistency of the APTS with other studies [7,27–30].

5.7. Phase relation between lithology and insolation

Lignite was previously argued to correspond to an insolation minimum, with cool summers, and marl to an insolation maximum, with warm summers. This preferred phase relation is particularly clear in intervals with alternating high- and low-amplitude insolation peaks, occurring at times of low eccentricity minima. The precession amplitude is then reduced, resulting in a relatively larger effect of obliquity on insolation. Such interference patterns are for example observed at ~4.45 Ma and 4.53 Ma. In these intervals, relatively high-amplitude minima and maxima are correlated to the thick lignites of T1 and T3 and to the thick marls of T1 and T2 respectively, and low-amplitude minima and maxima to the thin lignite of T2 and to the thin or absent marl of K27 respectively. No matching lithological and insolation patterns would be found in this interval if the inverse phase relation were used. The same holds for cycles K14–17 and N13–16, where some lignite and marl beds are more prominent or thicker than others and can only be correlated to insolation if the preferred phase relation is used.

In conclusion, organic material was preserved during periods with cooler summers (insolation minima), whereas marl was preferentially deposited during periods with warmer summers (insolation maxima). Combined sedimentological observations and gastropod assemblages [11] and preliminary palynological data (van Hoeve, pers. comm.) all suggest that lignite corresponds to a reed swamp environment, and marl to a relatively deeper lake. Hence,

the lake level was higher at times of increased summer insolation and lower at times of reduced summer insolation, implying that the amount of precipitation and related run-off dominated evaporation in controlling the lake level. This is in agreement with the inferred precipitation increase in the eastern Mediterranean northern borderlands during an insolation maximum, i.e. when the Earth resided in perihelion during boreal summer [31,32]. A similar humidity–temperature relation was found for marine environments in the Mediterranean during the Pliocene [33–35].

5.8. Eccentricity

The influence of precession on the lithology is evident in the Ptolemais sequence, but an expression of 100-kyr eccentricity is only found in the typical clustering of the uppermost ten cycles of the Notio member. A few other 100-kyr minima can be recognised as cycles with anomalous thickness and/or expression fitting the insolation curve (caused by the increased relative importance of obliquity). Expression of the 100-kyr cycles is especially lacking within the 400-kyr maxima around 5.05 and 4.6 Ma. In these intervals, the eccentricity time series shows little variation and/or relatively high minima (Fig. 5a), caused by a ~2 Myr-eccentricity cycle with a minimum at ~4.65 Ma.

The most pronounced 400-kyr minima in the Rossello composite section are found around 5.25 and 4.4 Ma. The very same intervals have an unusual lithology in Ptolemais: beige marls around 4.4 Ma and the lacustrine marls of the Lower Formation around 5.25 Ma. The Lower Formation marls, however, continue further downwards and are still found well below the 400-kyr eccentricity minimum, so, in addition to astronomically forced climate, other factors must have influenced the long-term changes in lithology.

5.9. Lower Thvera discrepancy

The polarity reversal horizons in Ptolemais typically deviate less than one i-cycle (i.e. less than half a lithological cycle) from the APTS, except for the lower Thvera, which differs three i-cycles, i.e. $1\frac{1}{2}$ lithological cycle (Table 1). Its position could be determined from the Tomea Eksi section as well as from the Komanos section. Although in the latter section the cyclic pattern was unclear below cycle K4, the reversal was recorded just above the volcanic ash layer dividing cycles K1 and 2, and well below the ash layer in lignite K3, thus confining the position to K2.

Since the Ptolemais age of the reversal is too young compared to the APTS, delayed acquisition in Ptolemais cannot explain the discrepancy. Therefore, we argue that the position of the lower Thvera in the Rossello composite might be too old. A close look at the results of Van Hoof and Langereis [36] from their detailed lower Thvera record in the Rossello composite, reveals that their two uppermost samples are reversed, indicating that the actual reversal horizon could be located higher in the stratigraphy than they interpreted.

6. Conclusions

A reliable magnetostratigraphy of the lacustrine deposits of Ptolemais has been established. Despite the occurrence of delayed acquisition of magnetic remanence, the difference in the positions of the reversal horizons between Ptolemais and the APTS/Rossello composite is less than half a lithological cycle (~10 kyr), except for the lower Thvera. The resulting time frame proves that astronomical forcing of climate determines the continental lacustrine environment, in particular through the influence of climatic precession.

The most important result of this study is the unprecedented accuracy of the correlation of continental (i.e. lacustrine) sequences to the marine realm through tuning to the insolation time series, a correlation we consider reliable on a bed-to-bed scale. Typical patterns co-occur in the same cycles and in the same climatic phases in both the continental and marine records, implying that the argued phase relation is correct, i.e. that lignites were deposited in dryer periods with cooler summers, and marls in more humid periods with warmer summers.

Thus, the results provide a highly accurate time frame, which will enable detailed and comparative palaeoclimate studies in both marine and continental environments.

Acknowledgements

We thank prof. dr. E. Velitzelos and prof. dr. C.S. Doukas for arranging necessary contacts and for their pleasant co-operation in the field. The field assistance and fruitful discussions with Marloes van Hoeve, Hans de Bruin, Hendrik-Jan Bosch, Konstantin Theocharopoulos, Wout Krijgsman and Mark Dekkers are much appreciated. We are grateful to the employees of the Public Power Company (ΔΕΗ/ΛΚΠ-A) for providing us with the freshest possible outcrops and digging 'staircases' to reach these outcrops. We thank N.J. Shackleton, W.A. Berggren and an anonymous reviewer for their valuable comments. The investigations were supported by the Netherlands Geosciences Foundation (GOA) with financial aid from the Netherlands Organisation for Scientific Research (NWO). This work was conducted under the programme of two Dutch national research schools: the Vening Meinesz Research School of Geodynamics (VMSG) and the Netherlands Research School of Sedimentary Geology (NSG). ***[RV]***

References

[1] C.G. Langereis, F.J. Hilgen, The Rossello composite: a Mediterranean and global reference section for the Early to early Late Pliocene, Earth Planet. Sci. Lett. 104 (1991) 211–225.

[2] F.J. Hilgen, Sedimentary cycles and high-resolution chronostratigraphic correlations in the Mediterranean Pliocene, Newsl. Stratigr. 17 (1987) 109–127.

[3] F.J. Hilgen, Astronomical calibration of Gauss to Matuyama sapropels in the Mediterranean and implication for the Geomagnetic Polarity Time Scale, Earth Planet. Sci. Lett. 104 (1991) 226–244.

[4] F.J. Hilgen, Extension of the astronomically calibrated (polarity) time scale to the Miocene/Pliocene boundary, Earth Planet. Sci. Lett. 107 (1991) 349–368.

[5] L.J. Lourens, A. Antonarakou, F.J. Hilgen, A.A.M. van Hoof, C. Vergnaud-Grazzini, W.J. Zachariasse, Evaluation of the Plio-Pleistocene astronomical time scale, Paleoceanography 11 (1996) 391–413.

[6] J. Laskar, The chaotic motion of the solar system: A numerical estimate of the size of the chaotic zones, Icarus 88 (1990) 266–291.

[7] N.J. Shackleton, S. Crowhurst, T. Hagelberg, N.G. Pisias, D.A. Schneider, A new late Neogene time scale: Application to Leg 138 sites, Proc. Ocean Drill. Program Sci. Results 138 (1995) 73–101.

[8] A. Berger, M.F. Loutre, Insolation values for the climate of the past 10 m.y., Q. Sci. Rev. 10 (1991) 297–317.

[9] D.V. Kent, P.E. Olsen, W.K. Witte, Late Triassic–earliest Jurassic geomagnetic polarity sequence and paleolatitudes from drill cores in the Newark rift basin, eastern North America, J. Geophys. Res. 100 (1995) 14965–14998.

[10] P.E. Olsen, D.V. Kent, B. Cornet, W.K. Witte, R.W. Schlische, High-resolution stratigraphy of the Newark rift basin (early Mesozoic, eastern North America), Geol. Soc. Am. Bull. 108 (1996) 40–70.

[11] J. Steenbrink, N. Van Vugt, F.J. Hilgen, J.R. Wijbrans, J.E. Meulenkamp, Sedimentary cycles and volcanic ash beds in the lower Pliocene lacustrine succession of Ptolemais (NW Greece): discrepancy between 40Ar/39Ar and astronomical ages, Palaeogeogr. Palaeoclimatol. Palaeoecol. in press, 1998.

[12] J.L. Mercier, D. Sorel, P. Vergely, Extensional tectonic regimes in the Aegean basins during the Cenozoic, Basin Res. 2 (1989) 49–71.

[13] S.B. Pavlides, D.M. Mountrakis, Neotectonics of the Florina–Vegoritis–Ptolemais Neogene basin (NW Greece): an example of extensional tectonics of the greater Aegean area, Ann. Geol. Pays Hell. 33 (1986) 311–327.

[14] G. Kaouras, Kohlenpetrographische, Palynologische und Sedimentologische Untersuchungen der Pliozänene Braunkohle von Kariochori bei Ptolemais/NW-Griechenland, Thesis Universität Göttingen, 1989.

[15] E. Ehlers, Bericht über die die bisher im Rhamen der Expertise Ptolemais durchgeführten geologischen und paläontologischen Untersuchungen, Bundesanst. Geowiss. and Rohst. Hannover, 1960, pp. 1–36.

[16] A. van de Weerd, Early Ruscinian rodents and lagomorphs (Mammalia) from the lignites near Ptolemais (Macedonia, Greece), Proc. K. Ned. Akad. Wet. B 82 (1978) 127–170.

[17] F. Gramann, Die Fossilien des Braunkohlenbeckens von Ptolemais–Komanos, Bundesanst. Geowiss. and Rohst Hannover, 1960, pp. 37–49.

[18] A.A.M. van Hoof, C.G. Langereis, Reversal records in marine marls and delayed acquisition of remanent magnetization, Nature 351 (1991) 223–225.

[19] M. Rossignol-Strick, African monsoons, an immediate climate response to orbital insolation, Nature 304 (1983) 46–49.

[20] F.J. Hilgen, W. Krijgsman, C.G. Langereis, L.J. Lourens, A. Santarelli, W.J. Zachariasse, Extending the astronomical (polarity) time scale into the Miocene, Earth Planet. Sci. Lett. 136 (1995) 495–510.

[21] C.G. Langereis, M.J. Dekkers, G.J. de Lange, M. Paterne, P.J.M. van Santvoort, Magnetostratigraphy and astronomical calibration of the last 1.1 Myr from an eastern Mediterranean piston core and dating of short events in the Brunhes, Geophys. J. Int. 129 (1997) 75–94.

[22] N.J. Shackleton, S. Crowhurst, Sediment fluxes based on an orbitally tuned time scale 5 Ma to 14 Ma, Site 926, Proc. Ocean Drill. Program Sci. Results 154 (1997) 69–82.

[23] C. Vergnaud-Grazzini, W.B.F. Ryan, M.B. Cita, Stable isotope fractionation, climatic change and episodic stagnation

in the eastern Mediterranean during the late Quaternary, Mar. Micropaleont. 2 (1977) 353–370.
[24] F.J. Hilgen, L.J. Lourens, A. Berger, M.F. Loutre, Evaluation of the astronomically calibrated time scale for the late Pliocene and earliest Pleistocene, Paleoceanography 8 (1993) 549–565.
[25] H. Loh, Die Genese und Fazies der quartaren Torf-Lagerstatte von Agras (Griechisch-Mazedonien) als Hintergrund der Braunkohlen-Mazeral- und Lithotypen-Bildung, Dissertation thesis, Georg-August-Universitat, Gottingen, 1992, 61 pp.
[26] S. Bottema, Late Quaternary Vegetation History of Northwestern Greece, Groningen, Groningen, 1974, 190 pp.
[27] D.S. Wilson, Confirmation of the astronomical calibration of the magnetic polarity time scale from sea-floor spreading rates, Nature 364 (1993) 788–790.
[28] P.R. Renne, A.L. Deino, R.C. Walter, B.D. Turrin, C.C. Swisherr, T.A. Becker, G.H. Curtis, W.D. Sharp, A.R. Jaouni, Intercalibration of astronomical and radioisotopic time, Geology 22 (1994) 783–786.
[29] C.M. Hall, J.W. Farrell, Laser $^{40}Ar/^{39}Ar$ ages of tephra from Indian Ocean deep-sea sediments: tie points for the astronomical and geomagnetic polarity time scales, Earth Planet. Sci. Lett. 133 (1995) 327–338.
[30] B.M. Clement, C.C. Swisher, P. Rodda, New magnetostratigraphic and $^{40}Ar/^{39}Ar$ dating results from the Suva Marl, Fiji: calibration of the Early Pliocene geomagnetic polarity time scale, Earth Planet. Sci. Lett. 151 (1997) 107–115.
[31] M. Rossignol-Strick, Rainy periods and bottom water stagnation initiating brine accumulation and metal concentrations: 1. The Late Quaternary, Paleoceanography 2 (1987) 333–360.
[32] E.J. Rohling, F.J. Hilgen, The eastern Mediterranean climate at times of sapropel formation: a review, Geol. Mijnb. 70 (1991) 253–264.
[33] J.P. de Visser, J.H.J. Ebbing, L. Gudjonsson, F.J. Hilgen, F.J. Jorissen, P.J.J.M. Verhallen, D. Zevenboom, The origin of rhythmic bedding in the Pliocene Trubi Formation of Sicily, Southern Italy, Palaeogeogr. Palaeoclimatol. Palaeoecol. 69 (1989) 45–66.
[34] B.J.H. van Os, L.J. Lourens, L. Beaufort, F.J. Hilgen, G.J. de Lange, The formation of Pliocene sapropels and carbonate cycles in the Mediterranean: diagenesis, dilution and productivity, Paleoceanography 9 (1994) 601–617.
[35] P.C. Tzedakis, Long-term tree populations in northwest Greece through multiple Quaternary climatic cycles, Nature 364 (1993) 437–440.
[36] A.A.M. van Hoof, C.G. Langereis, The upper and lower Thvera sedimentary geomagnetic reversal records from southern Sicily, Earth Planet. Sci. Lett. 114 (1992) 59–76.
[37] A. Papakonstantinou, Die hydrogeologischen Verhaltnisse im Raum der Ptolemais-Senke und die westlichen Vermiongebirges in Griechisch-Mazedonien, Berliner Geowiss. Abh. 13 (1979) 1–79.